Proton Transfer in Rubazoic Acid Derivatives in Solution and in the Solid State. An NMR Study

Alejandro C. Olivieri,[*,a,†] **Dionísia Sanz,**[b] **Rosa Mª. Claramunt**[b] **and José Elguero**[*,a]
[a] *Centro Nacional de Química Orgánica, Instituto de Química Médica, CSIC, E-28006 Madrid, Spain*
[b] *Departamento de Química Orgánica y Biología, Facultad de Ciencias, UNED, Ciudad Universitaria, E-28040 Madrid, Spain*

Solution ^1H and ^{13}C, and solid-state ^{13}C CPMAS NMR data are reported for the rubazoic acid derivatives 4-(5-hydroxy-1,3-dimethylpyrazol-4-ylmethylidene)-1,3-dimethyl-2-pyrazolin-5-one **1**, 4-(5-hydroxy-1,3-dimethylpyrazol-4-ylimino)-1,3-dimethyl-2-pyrazolin-5-one **2**, 4-(5-hydroxy-1-phenyl-3-aminopyrazol-4-ylmethylidene)-1-phenyl-3-amino-2-pyrazolin-5-one **3**, and 4-(5-hydroxy-1-*p*-sulfophenylene-3-methylpyrazol-4-ylmethylidene)-1-*p*-sulfophenylene-3-methyl-2-pyrazolin-5-one **4**. Solution ^{15}N NMR chemical shifts have also been measured. Isotopic ^2H shifts for the OH signal in $CDCl_3$ for the first two compounds were found to be $+0.28 \pm 0.03$ and $+0.40 \pm 0.03$ ppm respectively. AM1-calculated molecular geometries are also reported. The overall results support the idea of a fast proton transfer equilibrium between two enolic tautomers both in solution and in the solid state. The degeneracy of the tautomers is removed in crystals.

Proton transfer phenomena along intramolecular hydrogen bonds have been a matter of concern over the years.[1–3] In this regard, a considerable amount of work has been devoted to the study of enolic 1,3-diketones both in solution and in the solid state.[4–9] Spectroscopic techniques seem to favour the existence of a rapid tautomeric equilibrium **a** $\rightleftharpoons$ **b** (Scheme 1) in both phases,[4–9] whereas diffraction data has traditionally been interpreted in terms of a single delocalized skeleton **c**, or according to a 'resonance-assisted' hydrogen bond model **d** $\longleftrightarrow$ **e**.[10,11] However, recent analyses of thermal parameters derived from low temperature X-ray diffraction measurements seem to lend support to the idea of a fast proton transfer equilibrium **a** $\rightleftharpoons$ **b** in crystals.[12,13]

All enolic 1,3-diketones exhibit a highly deshielded ^1H NMR OH signal in almost all solvents, which lie in the range 13–18 ppm.[5] The measurement of the isotopic shift caused by replacement of the labile OH hydrogen by ^2H (or even by ^3H), *i.e.* the value of $\Delta = \delta(^1H) - \delta(^2H)$ has been used to distinguish between a double minimum potential well for the proton motion (corresponding to the tautomeric equilibration **a** $\rightleftharpoons$ **b**) for which Δ is expected to be positive, and a single minimum situation (corresponding to either **c** or **d** $\longleftrightarrow$ **e**) for which Δ should be negative.[5,14] In all 1,3-diketones hitherto studied, Δ was found to be positive and in the range from +0.3 to +0.7 ppm, pointing to a double well potential,[5] even in structures where steric congestion produced by bulky R^2 groups caused the oxygens to move close together and the OH proton to shift considerably downfield from the unsubstituted partners.[5,15] Only in certain charged structures, such as protonated 1,3-diketones or in monoanions of dicarboxylic acids, where the OH signals are at *ca.* 20–21 ppm, Δ was found to be negative, indicating a single minimum potential.[5] However this conclusion has been recently challenged, in the case of the latter species dissolved in water, in view of ^{13}C NMR data for ^{18}O enriched compounds.[16,17]

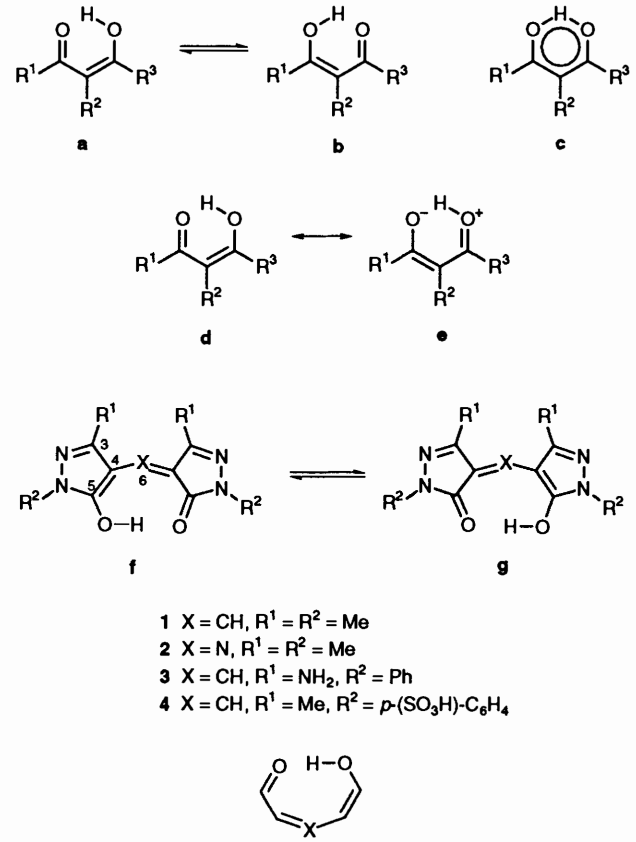

1 X = CH, $R^1 = R^2 = Me$
2 X = N, $R^1 = R^2 = Me$
3 X = CH, $R^1 = NH_2$, $R^2 = Ph$
4 X = CH, $R^1 = Me$, $R^2 = p\text{-}(SO_3H)\text{-}C_6H_4$

5 X = CH
6 X = N

Scheme 1

Rubazoic acid derivatives **1–4** (Scheme 1) are examples of enolic 1,5-diketones in which the OH participates in a strong hydrogen bond.[18–20] Observed O···O distances are in the range 2.42–2.45 Å,[21] comparable to the shortest values measured in 1,3-diketones (around 2.4 Å).[6,7,10,11] The special structure generated by the eight-membered H-chelated ring also shows a favourable O–H···O angle for strong hydrogen bonding which is near 180°.[21] Furthermore, ^1H NMR signals in $CDCl_3$ for a large variety of rubazoic derivatives resonates at $\delta = 17$–18, again in the upper range of values observed in 1,3-diketones.[20] These aspects make rubazoic acids interesting compounds to probe the nature of the proton potential energy

---

[†] *Permanent address:* Departamento de Química Analítica, Facultad de Ciencias Bioquímicas y Farmaceúticas, Suipacha 531, Rosario (2000), Argentina.

profile both in the liquid and solid states. In the present work, we report ^1H and ^{13}C NMR chemical shifts for 4-(5-hydroxy-1,3-dimethylpyrazol-4-ylmethylidene)-1,3-dimethyl-2-pyrazolin-5-one **1**, 4-(5-hydroxy-1,3-dimethylpyrazol-4-ylimino)-1,3-dimethyl-2-pyrazolin-5-one **2**, 4-(5-hydroxy-1-phenyl-3-aminopyrazol-4-ylmethylidene)-1-phenyl-3-amino-2-pyrazolin-5-one **3**, and 4-(5-hydroxy-1-*p*-sulfophenylene-3-methylpyrazol-4-ylmethylidene)-1-*p*-sulfophenylene-3-methyl-2-pyrazolin-5-one **4**, as well as ^2H isotopic shifts (Δ) for **1** and **2**, which support the existence of a double minimum potential (*i.e.* an equilibrium of the type $\mathbf{f} \rightleftharpoons \mathbf{g}$, see Scheme 1). ^{15}N NMR data are also reported in solution. Additionally, ^{13}C CPMAS NMR data are reported for solids **1–4**, with results which are similar to those found in solution, indicating that similar proton transfer phenomena occur in both phases. The molecular geometries obtained by optimization with the semiempirical MO program AM1 on compounds **1** and **2** and on their basic skeletons **5** and **6** (Scheme 1) are also discussed.

Experimental

All compounds were synthesized using known procedures.[18,19] Replacement of the OH proton in **1** and **2** by ^2H was achieved by heating the compounds in a mixture of $CDCl_3$ and D_2O, followed by evaporation and drying of the solid material under vacuum.

Solution ^1H, ^{13}C, ^2H and ^{15}N NMR measurements were made on a Bruker AC 200 spectrometer operating at nominal frequencies of 200.1, 50.3, 30.7 and 20.3 MHz respectively. Solid state ^{13}C NMR spectra were recorded on the same spectrometer at 50.3 MHz using a CPMAS accessory. Samples were packed in 7 mm ZrO_2 rotors and spun at 3.5–4.5 kHz. Typical spectral conditions were: SW, 20 KHz; ^1H 90° pulse, 7 μs; contact time, 3 ms; recycle delay, 1 s; number of acquisitions, 2000; memory, 1K; the chemical shifts are given with respect to the spectrometer reference frequency which was calibrated by the glycine signal at 176.1 ppm.

AM1 calculations were performed using the AMPAC package, version 2.10 with gradient optimization, in all cases with the PRECISE option.

Results and Discussion

Solution ^1H NMR data for **1–4** are given in Table 1. The appearance of a highly deshielded OH signal in $CDCl_3$ solution and the number of observed ^1H resonances in **1** and **2** are consistent with strongly hydrogen bonded structures (Scheme 1) displaying effective C_{2v} symmetries. A simple method to probe the nature of the proton potential energy profile is the measurement of the isotopic ^2H shift $\Delta = \delta(^1H) - \delta(^2H)$ for the OH signal. As previously discussed,[5,14] the heavier isotope tends to concentrate near the bottom of the energy well. If the system belongs to the double minimum type with a small internal barrier, ^2H will move towards one of the oxygen atoms and a relative shielding will be observed with respect to ^1H, *i.e.* Δ will be positive. Conversely, for single minimum structures, ^2H will move closer to the centre of the O • • • O line, and the resulting deshielding will lead to a negative Δ. The results for **1** and **2** are presented in Table 1, and in both cases a double minimum structure is supported, which is responsible for the effective symmetry observed in solution. ^1H NMR spectra for **1** and **2** were also recorded in $[^2H_6]$DMSO (Table 1), and similar results were obtained (although a broadening of the OH signal of **2** was observed). Due to low solubility in non-polar solvents, ^1H NMR spectra for compounds **3** and **4** were registered in $[^2H_6]$DMSO, with similar results to those discussed above for **1** and **2** (Table 1). This supports the idea that all compounds **1–4** have strong intramolecular hydrogen bonds where fast proton transfer between tautomers **f** and **g** takes place. Table 2 shows the ^{15}N NMR data recorded for **1**, **2** and **4** in solution. Due to the effective molecular symmetry of these compounds, single resonances for N(1) and N(2) are detected, in agreement with previous reports.[19]

Table 1 ^1H NMR chemical shifts in solution for compounds **1–4**[a]

Compound		$\delta_{^1H}$	
		$CDCl_3$	$[^2H_6]$DMSO
1	N-Me	3.46	3.39
	C-Me	2.21	2.21
	H(6)	7.08	7.32
	OH	17.81 ($\Delta = +0.28 \pm 0.03$)	17.84
2	N-Me	3.50	3.41
	C-Me	2.22	2.13
	OH	17.30 ($\Delta = +0.40 \pm 0.03$)	17.4 (br)
3[b]	H(6)		7.54
	H(2′,6′)		7.42 (t, *J* 8 Hz)
	H(3′,5′)		7.96 (d, *J* 8 Hz)
	H(4′)		7.16 (t, *J* 8 Hz)
4[b]	C-Me		2.36
	H(6)		7.51
	H(2′,6′)		7.72 (d, *J* 8 Hz)
	H(3′,5′)		7.83 (d, *J* 8 Hz)
	OH		17.8 (br)

[a] Δ is the isotopic shift $\delta(^1H) - \delta(^2H)$ for the OH signal. [b] The numbering 1′–6′ is for the phenyl rings carbons; C(1′) is attached to N(1).

Table 2 ^{15}N NMR chemical shifts in solution for compounds **1**, **2** and **4**[a]

Compound	N(1)	N(2)	=N–	Solvent
1	−197.2	−85.7		$CDCl_3$
2	−197.8	−82.5	−31.6	$CDCl_3$
4	−185.9	−92.4		$[^2H_6]$DMSO

[a] In ppm from NO_2CH_3.

^{13}C NMR chemical shifts in solution are reported in Table 3. Assignments were made by comparison with previously reported values for related compounds.[19] As can be observed, single, dynamically averaged resonances were observed for C(3), C(4), C(5), and the N-*Me* and C-*Me* groups in compound **1** both in $CDCl_3$ and in $[^2H_6]$DMSO, consistent with the structure shown in Scheme 1. The ^{13}C CPMAS spectrum of **1**, on the other hand, reveals splittings in carbons which are equivalent in solution due to the degeneracy of the interconverting tautomers **f** and **g** [N-*Me*, C-*Me*, C(4) and C(5)] whereas single peaks are obtained both for C(3) and C(6). Analysis of model compounds where tautomerism is absent[19] shows that the most sensitive chemical shift to changes in the equilibrium composition is that of C(4). The largest partition in the solid state (1.8 ppm) corresponds, as expected, to the chemical shift of C(4). (Similar results have been previously discussed for the CO carbons in 1,3-diketones.)[8,9] This can be explained on the basis of the loss of the effective solution symmetry in crystals. Compound **1** crystallizes in space group *Pnma*, with $Z = 4$, and the molecular plane coincides with a crystallographic mirror plane.[21] Relevant geometrical data are collected in Table 4. Although both halves of the molecule are not identical, the pairs of enolic C(5)–O, C(4)–C(5) and C(4)–C(6) bond lengths are very similar, indicating that if there is a deviation of the degenerate proton transfer $\mathbf{f} \rightleftharpoons \mathbf{g}$ in crystals, the latter must be small. Observed C(5)–O and C(4)–C(6) bond lengths are clearly averages of those expected for double and single bonds, as reported for 1,3-diketones.[11–13] The distance

Table 3 ^{13}C NMR chemical shifts in solution and in the solid state for compounds **1**–**4**

		δ_C		
Compound	Carbon	$CDCl_3$	$[^2H_6]$DMSO	Solid
1	N-*Me*	32.33	32.38	31.7, 33.1
	C-*Me*	12.50	12.34	12.9, 13.5
	C(3)	151.31	151.61	152.2
	C(4)	107.73	107.20	107.4, 109.2
	C(5)	161.31	160.76	159.1, 160.8
	C(6)	137.76	139.45	138.4
2	N-*Me*	33.01	32.95	33.5
	C-*Me*	11.70	11.37	12.3
	C(3)	152.82[a]	152.07[a]	151.5[a]
	C(4)	124.81	124.27	123.8, 124.6
	C(5)	153.17[a]	152.14[a]	152.5[a]
3[b]	C(3)		155.37	156.1
	C(4)		99.64	97.8, 103.9
	C(5)		162.81	159.8
	C(6)		146.21	147.0
	C(1′)		137.81	134.8, 136.5
	C(2′,6′)		118.95	117.1, 118.8
	C(3′,5′)		127.62	129.4
	C(4′)		123.07	122.5
4[b]	C-*Me*		12.69	12.9
	C(3)		153.84	155.1
	C(4)		109.06	103.7, 106.4, 108.3, 111.6
	C(5)		160.76	161.2
	C(6)		137.40	139.9
	C(1′)		140.28	139.9
	C(2′,6′)		119.78	118.4
	C(3′,5′)		126.50	126.9
	C(4′)		145.66	142.7

[a] Assignments may be interchanged. [b] C(1′–6′) belong to the phenyl rings; C(1′) is attached to N(1).

Table 4 Relevant distances within the enolic ring in compounds **1** and **2** according to X-ray diffraction

Compound		Distance[a]/Å	
1	C(5)–O	1.277, 1.276	
	C(4)–C(5)	1.440, 1.447	
	C(4)–C(6)	1.398, 1.384	
	O···O	2.425	
	O–H	1.120	
	O···H	1.306	
2[b]	C(5)–O	1.251, 1.260	1.280, 1.283
	C(4)–C(5)	1.470, 1.463	1.461, 1.472
	C(4)–N	1.325, 1.312	1.324, 1.305
	O···O	2.451	2.429
	O–H	1.067	0.864
	O···H	1.400	1.608

[a] Two values are given for C–C, C–O and C–N distances, corresponding to both halves of the molecules. All values have been taken from ref. 21. [b] Two independent molecules in the unit cell.

C(4)–C(5) seems however to be unusually long. The double C=C bond in the hydroxy tautomer of 1-phenyl-3-methylpyrazol-5-one is 1.36 Å, whereas in the pyrazolone tautomer the analogous C–C single bond is 1.40 Å.[22] Although C(4)–C(5) should be the formal average of comparable double and single bonds, it is even longer than the single bond value. This may be due to the needs of the congested eight-membered ring (see below). The X-ray structure of **1** also shows a single OH hydrogen, which is located slightly off-centre of the O···O line (Table 4), also a typical result for 1,3-diketones[5,11–13] for which diffraction data are unable to distinguish between a single hydrogen site with large thermal motion and two fractionally occupied sites which are close in space. Hence, the X-ray structure of **1** is consistent with the NMR information if the former is interpreted as the weighted average of both interconverting tautomers **1f** and **1g** which are slightly unequally populated in crystals.

Semiempirical AM1 calculations[23] were done on the eight-membered enolic ring of rubazoic structures. When the skeleton **5** is fully optimized, a non-planar structure results with dihedral angles of *ca.* 60° around both C–C single bonds. The calculated O···O distance (Table 5) is rather long, but similar to other AM1 optimized values in 1,3-diketones.[8,9,24] The remaining geometrical data (Table 5) shows the labile hydrogen clearly bonded to one of the oxygens, and an apparent alternation in bond lengths within the enolic ring. No abnormally large C–C bonds are obtained that could explain the observed C(4)–C(5) distance in compound **1**. It is interesting to notice that AM1 optimizes malondialdehyde, the lower vinilogue of **5**, yielding a planar structure consistent with experimental results.[24] However, when rubazoic acid **4** is fully optimized, both halves of the molecule are planar, while the dihedral angle around the single bond C(4)–C(6) is reduced to 33°. When the molecule is restricted to be planar, a geometry resembling the one found by diffraction measurements is obtained (Table 5). Furthermore, the calculated distances within the planar enol ring for the pairs of C(4)–C(5) bonds are significantly longer than those for C(4)–C(6) bonds. The averages of C(5)–O, C(4)–C(5) and C(4)–C(6) bond lengths (which would result if both tautomers were equally populated in the solid state) are 1.296 Å, 1.456 Å and 1.379 Å, in better agreement with the experimental data (Tables 4 and 5). The calculated heats of formation for the fully optimized structure and for the planar one are +58.6 and

Table 5 Relevant AM1 calculated geometrical data for **1**, **2**, **5** and **6**

Compound		Distance[a]/Å	
5	C(5)–O	1.234, 1.358	
	C(4)–C(5)	1.346, 1.464	
	C(4)–C(6)	1.339, 1.443	
	O···O	2.757	
	O–H	0.973	
	O···H	2.110	
1[b]	C(5)–O	1.241,1.354	1.242,1.349
	C(4)–C(5)	1.419,1.492	1.423,1.489
	C(4)–C(6)	1.344,1.416	1.347,1.411
	O···O	2.864	2.837
	O–H	0.977	0.975
	O···H	1.954	1.862
6	C(5)–O	1.231, 1.359	
	C(4)–C(5)	1.353, 1.487	
	C(4)–N	1.280, 1.391	
	O···O	2.848	
	O–H	0.971	
	O···H	2.108	
2[b]	C(5)–O	1.238,1.357	1.240,1.350
	C(4)–C(5)	1.428,1.521	1.437,1.517
	C(4)–N	1.282,1.366	1.280,1.349
	O···O	2.817	2.848
	O–H	0.978	0.974
	O···H	1.968	1.881

[a] Two values are given for C–C, C–O and C–N distances, corresponding to both halves of the molecules. [b] The first set of values corresponds to the fully optimized geometry; the second one to a structure restricted to planarity (see text).

+60.8 kcal mol^{-1} * respectively. The difference of only 2.2 kcal mol^{-1} could be easily surmounted by crystal packing forces in order to yield the observed planar structure in crystals.

Similar results to those discussed above were obtained for **2**. Solution ^{13}C NMR chemical shifts in both solvents are comparable (Table 3), and are indicative of a dynamic average between two degenerate tautomers **f** and **g**. CPMAS data show single peaks for all carbons (Table 3) with chemical shifts which are comparable to those measured in solution. An exception is the doubling in the equilibrium-sensitive carbon signal of C(4) (splitting = 0.8 ppm). Crystals of **2** belong to space group *Pbca*, with $Z = 16$, and there are two nearly planar, non-equivalent molecules within the unit cell.[21] As with **1**, the molecular geometry is deviated from the effective solution symmetry (Table 4), although only slightly. The pairs of analogous bond distances within the enolic ring are very similar [both C(4)–C(5) bonds appear to be rather long, as in **1**], while the labile OH hydrogen appears to be bonded to one of the oxygens in both independent molecules. Therefore, the doubling detected in the solid-state NMR signal of C(4) may be either due to a slight deviation from equipopulation on crystallization, or to the presence of non congruent molecules in the unit cell.

As before, full geometry optimization of the basic skeleton **6** yields a non-planar molecule with dihedral angles of *ca.* 60° about both C–C single bonds. On the other hand, **2** is fully optimized to a structure which is very similar to that of **1** [a dihedral angle of 34° is computed around the single C(4)–C(6) bond], except for both C(4)–N distances, as expected (Table 5). Restricting **2** to planarity gives a structure where the OH hydrogen is clearly bonded to one of the oxygens, while bond lengths within the enolic ring alternate between single and double (Table 5). AM1 calculated heats of formation are +71.4 kcal mol^{-1} (fully optimized geometry) and +73.8 kcal mol^{-1} (planar). Thus, similar arguments to those discussed above could be used in support of the observed planarity of **2** in crystals. If tautomers **2f** and **2g** were present in equal amounts at equilibrium, average enolic bond distances would be: C(5)–O, 1.295 Å; C(4)–C(5), 1.477 Å and C(4)–N, 1.314 Å, again in agreement with the X-ray structure (Table 4).

No diffraction data are available for **3** and **4**. ^{13}C and ^{15}N NMR results in [^{2}H$_6$]DMSO (Tables 2 and 3) are similar to those for **1** and **2**. This is indicative of a close similarity in the structures of these compounds in both phases, again indicating dynamically averaged chemical shifts due to the fast equilibrium **f** $\rightleftharpoons$ **g**. Doublings of some of the carbons' signals in the solid state [particularly C(4), see Table 3] could be due to changes in the tautomeric composition on crystallization. If this were the case, the partition observed for C(4) in **3** (6.1 ppm) may be an indication of a significant deviation from equipopulation in going from solution to the solid state. In the case of the CPMAS spectrum of **4**, four resonances were detected in the range expected for C(4) (Table 3). However, other sources of inequivalence, such as the presence of inequivalent molecules in the unit cell, or differential twisting angles of the phenyl rings with respect to the enolic ring cannot be discarded.

Conclusions

Solution ^{1}H, ^{2}H, ^{15}N and ^{13}C NMR information for four rubazoic acid derivatives is consistent with a fast degenerate proton exchange between two enolic tautomers. Solid-state ^{13}C NMR data are also in agreement with the presence of this equilibrium in crystals, although the degeneracy in solution seems to be removed in going to the solid phase. AM1-calculated geometries help to understand the observed crystal structure of these compounds.

Acknowledgements

One of us (A. C. O.) is indebted to *DGICYT* of Spain for financial support during his stay at the *Centro Nacional de Quimica Organica* of *CSIC*, and to *CONICET* (*Consejo Nacional de Investigaciones Cientificas*, Argentina) and *Universidad Nacional de Rosario* for a leave of absence. Thanks are given to *DGICYT* (Spain) for financial support (project PB 90-226-CO2). We thank Dr. Sebastian Cerdán (*Instituto de Investigaciones Bioorgánicas*, *CSIC*, Spain) for assistance in recording the ^{2}H NMR spectra.

References

1 W. C. Hamilton and J. A. Ibers, *Hydrogen Bonding in Solids*, W. A. Benjamin, New York, 1968.
2 M. D. Joesten and L. J. Schaad, *Hydrogen Bonding*, Marcel Dekker, New York, 1974.
3 P. Schuster, G. Zundel and C. Sandorfy, eds., *The Hydrogen Bond. Recent Developments in Theory and Experiments*, North Holland, Amsterdam, 1976.
4 Z. Rappoport, ed., *The Chemistry of Enols*, Wiley, Chichester, 1990.
5 F. Hibbert and J. Emsley, *Adv. Phys. Org. Chem.*, 1990, **26**, 255.
6 J. Emsley, *Chem. Soc. Rev.*, 1980, **9**, 91.
7 J. Emsley, *Struct. Bonding (Berlin)*, 1984, **57**, 147.
8 A. J. Vila, C. M. Lagier and A. C. Olivieri, *J. Chem. Soc., Perkin Trans. 2*, 1990, 1615.
9 A. J. Vila, C. M. Lagier and A. C. Olivieri, *J. Phys. Chem.*, 1991, **95**, 5069.
10 See ref. 4, ch. 13.
11 V. Bertolasi, P. Gilli, V. Ferretti and G. Gilli, *J. Am. Chem. Soc.*, 1991, **113**, 4917.
12 A. J. Vila, C. M. Lagier and A. C. Olivieri, *J. Mol. Struct.*, 1992, **274**, 215.
13 F. K. Larsen, M. Blomberg and G. M. Reisner, American Crystallography Meeting, Seattle, WA, July 1989, Abstract PB08;

---

* 1 cal = 4.184 J.

F. H. Herbstein, M. Kapon, G. M. Reisner and F. K. Larsen, 6th Gentner Symposium on Chemistry, Eilat, Israel, September 1989.
14 L. A. Altman, D. Laungani, G. Grunnarsson, H. Wennerstrom and S. Forsen, *J. Am. Chem. Soc.*, 1978, **100**, 8264.
15 A. M. Polozov, A. V. Khotinen, E. N. Klimovitskii, O. N. Kataeva and I. A. Litvinov, *J. Mol. Struct.*, 1992, **275**, 171.
16 C. L. Perrin and J. D. Thoburn, *J. Am. Chem. Soc.*, 1989, **111**, 8010.
17 C. L. Perrin and J. D. Thoburn, *J. Am. Chem. Soc.*, 1992, **114**, 8559.
18 W. Hänsel, *Justus Liebig Ann. Chem.*, 1976, 1380.
19 W. Hänsel, *Justus Liebig Ann. Chem.*, 1976, 1680.
20 S. Bratan-Mayer, F. Strohbusch and W. Hänsel, *Z. Naturforsch.*, 1976, **31b**, 1106.
21 U. Drück and W. Littke, *Acta Crystallogr., Sect. B*, 1980, **36**, 3002.
22 F. Bechtel, J. Gaultier and C. Hauw, *Cryst. Struct. Commun.*, 1973, **3**, 469.
23 M. J. S. Dewar, E. G. Zoebisch, E. F. Healy and J. J. P. Stewart, *J. Am. Chem. Soc.*, 1985, **107**, 3902.
24 See ref. 4, ch. 1.

Paper 3/02391E
Received 26th *April* 1993
Accepted 13th *May* 1993